Final Draft
of the original manuscript:

Polyethersulfone electrospun nanofibrous composite membrane for liquid filtration

S.Sh.Homaeigohar, K. Buhr, K.Ebert[a*]

Institute of Polymer Research
GKSS Research Centre Geesthacht GmbH, Max-Planck-Str. 1, 21502
Geesthacht, Germany

[a] present address: Institute of Materials Research
GKSS Research Centre Geesthacht GmbH, Max-Planck-Str. 1, 21502
Geesthacht, Germany

* To whom correspondence should be addressed:
Tel: (+49)4152-87-2476, E-mail: katrin.ebert@gkss.de

Abstract

        A Polyethersulfone (PES) electrospun nanofiber mat was evaluated as a membrane for liquid filtration. To alleviate difficult handling of the nanofibrous web and also to provide mechanical strength, Poly(ethylene terephtalate) (PET) non-woven was used as the sub layer. To enhance the interfacial stability, a heat treatment was performed. The PES/PET electrospun nanofibrous membranes (ENMs) were characterized in terms of water flux and retention performance. The water flux measurements indicated that the membranes possess a high permeability, but increase of feed pressure deforms the structure of the nanofibrous layer. This deformation decreases the effective porosity and as a result the permeation flux. Heat treatment approach in addition to enhancement of interfacial stability, could preserve the structure of the nanofibrous layer and its effective porosity. Retention tests based on Polystyrene suspension demonstrated that the filtration performance of the ENMs is highly dependent on size distribution of the suspended particles. When the particles over 1 μm in size (microparticles) are present in the feed, the major rejection of the particles is performed within the first hour of the measurement. Permeation flux is very high and pressure difference very low and almost negligible. In the case of a feed containing only nanoparticles (<1 μm in size), the major rejection is accomplished within the first hour, while it is completed after few hours. Nevertheless, the permeation flux declines and pressure difference rises drastically in less than 1 hour. This research demonstrated the filtration potential of this electrospun nanofibrous membranes for pre-treatment of water and also for other liquid separations.

Keywords: Electrospinning, nanofibers, liquid filtration, Polyethersulfone, pre-filter

1. Introduction

The electrospining technique is a well-known process for making continuous sub-micron to nano-size fibers in the nonwoven mat form. In this process, a high voltage is applied to the anode, immersed in the spinning solution. When the electrical force is higher than the surface tension of the solution, a charged jet of fluid is produced. Before, reaching the collecting screen, the solvent evaporates and the polymer is collected as an interconnected web of small fibers [1–4]. This nanofibrous web is highly porous with interconnected pores in the size range of only a few times to a few ten times the fiber diameter. The promising structural features makes the nanofibrous mat a suitable candidate for filtration applications. The high porosity implies a higher permeability and the interconnected pores can withstand fouling better. Besides, small pore size of the nanofibrous non-wovens results in a higher retention [5].

In separation technology, application of electrospun nanofibrous mats can be classified as three major areas: gas, liquid and molecular filtration. As air filters, electrospun nanofibrous non-wovens have been used commercially over the last 20 years [5]. However, in other filtration areas the research is extensively being done to meet the requirements for industrialization of such nanofibrous filters.

For liquid filtration, conventional porous polymeric membranes have their intrinsic limitations, e.g. low-flux and high-fouling performance. These drawbacks are due to the geometrical structure of pores, the corresponding pore size distribution [6] and undesirable macro-void formation across the whole membrane thickness [7]. It appears that the electrospun nanofibrous membranes can overcome some of these limitations [8]. For instance, Yoon et al. [8] and Wang et al. [9] have shown that

porous electrospun nanofibrous scaffolds can be used to replace flux limiting asymmetric porous ultrafiltration membranes.

In the current study, a PES electrospun nanofibrous mat was evaluated as a pre-filter in water treatment. In filtration, pre-filters are used to remove coarser particles, and maintain the performance of the down stream filter unit for much longer times before cleaning and/or replacement [10]. Compared to the conventional fibrous pre-filters, the nanofibrous ones at same areal density can offer very small pore sizes thus allowing a higher retention. Recently, Aussawasathien et al. [10] and Gopal et al. [11,12] have explored the viability of developing nylon-6, polyvinylidene fluoride and polysulfone pre-filters via the electrospinning process. Their applicability in particulate removal from monodisperse suspensions has been demonstrated. Such electrospun membranes have been successful in eliminating more than 90% of the micro-particles from suspension [10].

In our study, PES was selected as the membrane material due to its high thermal and chemical resistance, and also its appropriate mechanical properties. Besides, PES can be considered as a model membrane material as it is widely used for commercial microfiltration and ultrafiltration membranes.

Accumulation of electrostatic charges during the electrospinning is a problem which makes the handling of electrospun nanofibrous mats difficult. Spinning the nanofibers directly over a stronger, more rigid support is one way of alleviating the handling issue [11]. In the current study, to address the handling problem of the PES electrospun nanofibrous mat and to provide mechanical strength, a Poly(ethylene terephthalate) (PET) technical non-woven was employed as a sub layer. The schematic diagram of the composite membrane is illustrated in Fig. 1. Delamination is a problem which should be controlled in layered composite systems such as the

PES/PET composite membrane. To overcome delamination, a heat teatment approach was adopted in our study.

PES/PET electrospun nanofibrous membranes were characterized through water flux measurements. Besides, particulate suspension based retention tests were conducted to understand their capability and performance. To provide a more realistic situation compared to similar researches, we evaluated the retention capability of the nanofibrous composite membranes using a heterodisperse suspension for a longer time (i.e. 24 hours).

2. Experimental

2.1 Material

Polyethersulfone Ultrason E6020P (M_w= 58000 and density of 1.37 g/cm^3) was purchased from BASF (Germany). As the sub layer of the membrane, a technical PET non-woven was used. The solvent N,N-dimethylformamide (DMF) was obtained from Merck (Germany). All materials were used as received.

2.2 Electrospinning

PES/PET nanofibrous membranes were produced by an electrospinning method. Briefly, prepared PES solution (20 wt%) in DMF was fed with a constant rate of 0.5 ml/h into a needle by using a syringe pump (Harvard Apparatus, USA). By applying a 20kV voltage (Heinzinger Electronic GmbH, Germany) PES was electrospun on Aluminum foil (as the control substrate) and PET non-woven. The electrospinning conditions are tabulated in table 1.

2.3 Characterization of PES nanofibrous mat

The morphology of the PES electrospun fibers (electrospun on Aluminum foil) was observed through scanning electron microscope (SEM) (LEO 1550VP Gemini from Carl ZEISS). The diameter of the nanofibers was determined from the SEM images using the Adobe Acrobat v.07 software. The thickness of the PES nanofibrous mat after peeling off of Aluminum foil was measured using a digital micrometer (Deltascope® MP2C from Fischer).

The nanofibrous PES/PET mats were stamped out as circular with a diameter of 46 mm. The weight of the samples was measured using a laboratory electronic weighing balance (accuracy: 0.001 g). Based on the area and weight, the approximate areal density of the composite nanofibrous membranes was determined.

2.4 Heat treatment

A set of the samples was heated in the oven (Heraeus Vacutherm, max T=200°C) at the temperature of 190 °C for 6 hours in air and then were slowly cooled in the oven. The selected temperature is above the boiling point of the solvent (T_B(DMF)=153 °C) and below the glass transition temperature of PES (225 °C).

The interface between the PES nanofibers and PET microfibers was observed optically by SEM. Probable changes in the surface chemical properties of the PES nanofibers after heat treatment were investigated by Fourier Transform Infra Red Spectrometry (FTIR). Attenuated total reflection Fourier transform infrared (ATR-FTIR) spectra were recorded using a Bruker Equinox55 spectrometer.

The thermal properties and content of the solvent remaining in the electrospun fiber web were analyzed with a thermogravimetric analyzer of Netzsch 209 TG. TGA

analysis was performed at 20–450 ∘C with a heating rate of 10 ∘C/min under Ar condition.

2.5 Membrane characterization

2.5.1 Pore size distribution

Average pore size of the electrospun nanofibrous membranes was measured using a 500PSI automated capillary flow porometer from Porous Materials Inc.(PMI,USA). The stamps of the PES/PET nanofibrous membranes were immersed in the wetting fluid Porewick[®] from PMI (surface tension = 16×10^{-5} J/cm (16 dyn/cm)) for at least 10 min and then placed in the test cell with an effective area of 4.9 cm^2. Then by an automated procedure, a successively increasing pressure is applied across the nanofibrous membranes using nitrogen as pressurising gas. When the applied N_2 pressure exceeds the capillary attraction of the liquid in the pores, gas will pass through the sample. Smaller pores have a higher capillary attraction than larger pores and thus smaller pores open up at higher pressures. Bubble point is the point when the largest pore is opened up by the gas. So the bubble point pore diameter is the largest pore diameter of the sample. Besides, the mean flow pore diameter is computed from mean flow pressure. The mean flow pore diameter is such that 50% of flow is through pores larger than the mean flow pore diameter and 50% of flow is through pores smaller than the mean flow pore diameter.

The measurements were repeated three times using new samples. Sample to sample mass variation was less than 10%.

The Permeability and structural stability (integration) of the electrospun nanofibrous membranes (ENMs) were studied by water flux measurements. Circular ENMs 46 mm in diameter as un- and heat treated in two arrangements of single and an arrangement of 5 layers, later in the text referred to as multi layer, were used for permeability characterization. The latter arrangement was seen as a model for cartridge filters. A custom-built dead-end filtration set-up was designed for permeability and also retention characterizations which is shown in Fig. 2. The dried membrane was placed in the membrane cell and the water in the reservoir (500 ml distilled water) was circulated by a pump through the membrane cell. The flux measurements were performed at special time intervals including 0,1,3,5,7 and 24 hours. At the time intervals also the pressure difference (ΔP) between up and down stream sides of the membrane was recorded. To measure the water flux, the time needed to permeate 200 ml water through the membranes was recorded and the permeation flux was calculated by equation 1:

$$J = \frac{Q}{A.\Delta t} \qquad\qquad (1)$$

where J is the permeation flux (L/m^2.h), Q is the permeation volume (L) of water, A is the effective area of the membranes (m^2), and Δt is the sampling time (h). The flux measurement test was repeated three times.

2.5.3 Retention (Particle challenge test)

The retention capability of the PES/PET ENMs was determined using Polystyrene suspensions in two ranges of particle size (micron and sub-micron).

2.5.3.1 Suspension preparation

As the feed system for retention test, aqueous suspensions containing Polystyrene (PS) particles in two different average particle size including nano (submicron) and micron (1- 2 micron) were prepared via nano-precipitation technique [13]. For the preparation of the nanoparticles, we used a technical approach patented by Ebert et al. [14]. Polystyrene (Mw=100k) (Avocado Research Chemicals Ltd., UK) (0.1 wt%) was dissolved in tetrahydrofuran (THF) (Merck, Germany) and as the surfactant solution, Pluronic F-68 (2.5 g/L) (Sigma, USA) was dissolved in water. By mixing the two solutions, PS particles precipitate in water and the surfactant inhibits growth and agglomeration of the particles. THF is removed from the suspension in a rotational evaporator (rotavapor BÜCHI 461, Switzerland).

The particle size distribution was determined by using a particle size analyzer (Delsa C™ Nano particle size analyzer, Beckman Coulter, USA).

2.5.3.2 Retention test

Retention performance of the PES/PET membranes was determined at different time intervals (0,1,3,5,7 and 24 hours). The reservoir of the custom-built set-up (fig.2) was filled with 500 mL PS suspension as the feed. At the mentioned intervals, 100 mL permeate was taken to be analyzed by the particle size analyzer. As a measure for the retention ability the d90 was chosen. The d90 is a value of the particle size distribution representing the 90 % of the particles having a lower particle size. Besides, the time required for permeation (permeation flux) and also the pressure difference (ΔP) were recorded. The retention test was repeated three times using new PS suspensions with similar d90s (less and over 1 micron).

3. Results and Discussion

3.1 Characterization of PES nanofibrous mat

The morphology of the electrospun nanofibers is shown in fig 3. The surface of the nanofibers is relatively smooth and no beads and droplets is observed in the nanofibrous mat within the area inspected by SEM. Other properties of the PES nanofibrous mat are tabulated in table 2.

3.2 Heat treatment

The main concern in preparation of the composite membranes is creating a stable interface between the supporting and the nanofibrous layers. Hence, in our study a heat treatment approach was adopted to enhance the interfacial stability of the ENMs. It is assumed that the residual solvent in the nanofibers can partially re-dissolve PES by heating. Continuous heating results in diffusion of the solution outward of the nanofibers to the interface with PET microfibers. By evaporation of the solvent at the interface, the nanofibers and microfibers stick to each other firmly. The improved adhesion at the interface is clearly seen in SEM pictures (fig.4).

The ATR-FTIR spectra of the PES nanofibers before and after heat treatment, are shown in fig.5. Also the band assignments for the infrared spectrum of PES are shown in table 3. As can be seen in fig.5 no obvious difference between the spectra of the PES nanofibers heat treated in air and un-treated is observed. This means that heat treatment in air can not oxidize the nanofibers. Considering the difficulties and expenses of heat treatment under vacuum, this result can be very promising for application of such membranes on industrial scale.

As can be seen in fig.5, the only difference between the spectra of the heat- and un-treated nanofibers is the peak seen at 1671 cm^{-1} for the un-treated nanofibers. This

peak which disappears after the heat treatment, is related to carbonyl vibration of N-C=O group caused by the remaining solvent DMF [16]. The FTIR results imply that by heat treatment, surface chemical properties of the nanofibers do not change significantly.

Based on the TGA curves (fig.6), at the heat treatment temperature (190°C), weight reduction of the un-treated PES nanofibers is around 2.5%. This amount for the as received PES and the heat treated PES nanofibers are 0.6% and 0.8%, respectively. Evaporation of DMF is the main reason for loss of weight in the un-treated nanofibers within the studied range of temperature.

3.3 Membrane characterization

Different characteristics of the PES/PET nanofibrous membranes are tabulated in table 4.

3.3.1 Pore size distribution

Based on the bubble-point method, pressure is applied to the membrane base. At each pressure, the corresponding bubble (gas) flow rate is measured. The relationship between the pore size and the corresponding pressure is given by the Young-Laplace equation (2):

$$r = \frac{2\gamma}{\Delta P} \cos\theta \quad (2)$$

where r is radius of the pore, ΔP pressure difference, γ the surface tension of the wetting agent and θ the wetting angle (for the completely wetted membrane by the fluid, $\cos\theta = 1$). From the experiment, 'bubble-point' occurred at 0.1 bar,

corresponding to 5 µm pore size as determined using Eq. (2). Mean flow pore diameter was equal to 2 µm. This range of pore size in the PES nanofiber mat is in accordance with typical characteristics of microfiltration (MF) membranes [17].

3.3.2 Permeability

Pure water flux measurements were performed to demonstrate the permeability and structural stability of the PES/PET ENMs as single and multi (5) layer.

As can be seen in fig.7A, the pure water flux measured for the single layer un- and heat treated PES/PET membranes is high and comparable with the primary feed rate ($\approx 60 \times 10^3$ L/h.m^2). In both the cases, the flux is almost constant throughout the test.

Besides, as it is observed in fig.7B, ΔP for the single layer un- and heat treated PES/PET membranes is very low (≈ 50-170 mbar; at the start and the end of measurements, respectively) and virtually steady until the end of measurements.

According to Darcy's law [18,19,20], the flux of dead-end MF can be expressed as follows (equation 3):

$$J = \frac{k.\Delta P}{\mu.\Delta x}$$ (3)

Where J is the water flux (m/s) ($\approx 0.9 \times 10^6$ L/h.m^2); k: the permeability coefficient (m^2), ΔP: the pressure difference (Pa)($= 10^{-5}$ bar), µ: the viscosity (Pa.s), and Δx: the membrane thickness (m).

According to equation 3, considering viscosity (µ) of water and thickness (Δx) of the membrane as constant, high and constant flux (J) in addition to low and constant pressure difference (ΔP) implies a very high and constant permeability (k).

Hence, for both the un- and heat treated PES/PET membranes as single layer, permeability is very high and constant throughout the test. The constant permeability of the ENMs demonstrates that the nanofibrous layer is quite stable and the porosity does not change during filtration. This stability is due to low ΔP by which water flow does not change the structure of the nanofibrous layer.

In the case of the multi layer model, as can be seen in figs. 7A and B, water flux and ΔP for the un-treated PES/PET membrane has a decreasing and increasing trend, respectively, with a steep slope by the end of measurements. According to Darcy's law (equation 2), these variations indicate that the permeability of the ENMs as multi layer is decreasing.

The reason as can be seen in the SEM pictures (fig.8A) is deformation of the nanofibrous layer at higher pressure differences of about 817-1350 mbar (at the start and the end of measurements, respectively). The higher thickness of the multi layer membranes compared to the single layer ones results in a higher ΔP. The high ΔP leads to higher compressive and shear forces applied by water flow on the nanofibrous layer which results in its deformation at surface and bulk (compaction). The deformation reduces the interconnectivity of the pores, clogs the pores, decreases the effective porosity and as a result permeability of the membrane. As can be seen in figs.8 A-C, the deformation happens only on the uppermost nanofibrous layer. Different pattern of water flow on the uppermost layer compared to the other next layers is most probably the main reason for occurrence of deformation only on this layer. In addition, the uppermost layer acts as a damping layer for the next layers via absorption of the majority of mechanical stresses applied by water flow.

It should be noted that the formation of beads and droplets visible on the nanofibrous mat is mainly due to the non-conductivity of the PET non-woven which

decreases the electrical driving force for electrospinning. In this case, unlike electrospinning on Aluminum foil (fig.3), privilege of surface tension of the polymer solution on electrical force facilitates formation of defects such as beads and droplets.

In contrast to the un-treated PES/PET membranes, the heat treated ones maintain their steady trend of water flux and ΔP throughout the measurements. This shows that heat treatment can preserve the fibrous media and prevent its deformation. Similar to the mechanism involved in improvement of the interfacial stability, the residual solvent may stick the nanofibers to each other (fig.9). The interfiber adhesion makes the nanofibrous layer more resistant against compressive and shear stresses applied by water flow during filtration and as a result the deformation is prevented. As it is observed in SEM pictures (fig.10) after 24 hours filtration, the surface and bulk deformation (compaction) do not occur in the heat treated ENMs.

3.3.3 Retention (Particle challenge test)

The filtration performance of the PES/PET ENMs as single layer was investigated using a simple model based on Polystyrene (PS) aqueous suspension. Retention performance, pressure difference and permeation flux were characterized for the ENMs.

As mentioned earlier, d90 means the diameter below which 90% of particulate population lie, is the indication of retention performance of the ENMs. It should be noted that the polydispersity index (PI) values of all the primary suspensions used as feeds varied between 0.2 and 0.5 representing a broad dispersion of particle size [21]. This broad dispersion simulates actual characteristics of the feeds in pre-treatment of water.

As can be seen in fig.11, the retention performance of the ENMs is highly dependent on the size distribution (d90) of the suspended particles present in the feed. When d90 is closer to the average pore size of the ENMs and over 1 μm, the membranes are able to reject the particles based on their size after 1hour. The d90 of the particles in the primary feed is 1140 nm but after 1hour in the first permeate, this size decreases to approximately 600 nm. The rejection is not completed even after 24 hours and still there are particles present in the permeate with a d90 close to the d90 of the first permeate (fig.11A). This means that the bigger particles are rejected very soon within the first hour while smaller particles pass through the membranes by the end of measurements. This rejection performance is along with a high permeability (fig.11B) and very low pressure difference (fig.11C). This behavior can be very promising, if we consider the ENMs as a pre-filter.

In contrast to the suspensions with d90 in micron scale, when d90 significantly drops below the average pore size (560 nm), the ENMs reject all the nanoparticles after 5 hours while the major rejection of the nanoparticles is performed after 1 hour (fig.11A). In this case the high rejection efficiency of the membranes costs drastic decline of permeation flux (fig.11B) and increase of pressure difference (fig.11C) in a very short time (less than 1 hour).

The retention results are in agreement with what was obtained by Gopal et al [11] for monodisperse suspensions. They state that when the 10 μm particle suspension is used, retention by the nanofibrous membrane (average pore size of 4-10 μm) is less than that for the 1μm particle suspension (separation factors of 96% and 98%, respectively). In the case of flux, when the bigger particles are involved the flux is recovered completely indicating no permanent fouling of the membrane. In

contrast, for the 1μm particle suspension, the flux reduction is instantaneous at the onset of the experiment.

By a closer look at the surface of the ENMs with low permeation flux through SEM pictures, it is seen that the surface has been covered by a dense layer of particle deposits or so-called "cake layer" (figs.12 A and B). The PS nanoparticles are captured by the nanofibers (physical trapping). Besides, due to their very small size they pack closely together and form a cake layer. The cake layer clogs the pores of the ENMs significantly at the surface. Similarly, this behavior has been observed by Gopal et al. [11,12]. This situation as can be seen in figs. 12C and D does not occur when d90 is bigger than 1 μm and the dense cake layer does not form.

It should be noted that when the particle size is between 0.1 and 1 μm, due to the superimposition of brownian diffusion, lateral migration and shear induced diffusion, the velocity of particle migration away form the surface reaches to its minimum [22]. This theory explains the severe particle deposition observed in the ENMs when the particle size drops below 1μm. The cake layer caused the ENM to be irreversibly fouled and the initial flux could not be recovered. It is assumed that immediately at the start of experiment, the nanoparticles are trapped by the nanofibers and act as the initiation points for cake layer formation. The development of the cake layer takes place almost immediately and consequently the permeation flux declines drastically already at the onset of the experiments. In addition, this dense cake layer acts as the separating layer for the ENMs, resulting in significantly higher rejection of the nanoparticles in a very short time.

On the other hand, however, when d90 is over 1 micron (1140 nm), based on a PI indicating a broad distribution, there is a mixture of particles in micrometer and nanometer scale. It is assumed that the concentration of microparticles prevails on that

of nanoparticles. If the opposite case was true, we could expect formation of a dense cake layer such as what was observed for the suspensions with d90≈560 nm and subsequently flux decline. But, this situation never occurs. Hence, microparticles are rejected by the ENMs even though their respective size is smaller than the average pore size of the membranes. Here, the main mechanism for filtration of microparticles is assumed to be inertial impaction. Inertial impaction occurs when a particle is so large that it is unable to quickly adjust to the abrupt changes in streamline direction near a membrane. The particle, due to its inertia, will continue along its original path and hit the membrane.

When particle size and the number of particles increase, so does the probability of collision. As the particles collect, they themselves become part of the filter media, thereby increasing efficiency by adding to the number of possible collisions for other suspended particles. Through this mechanism, the microparticles are rejected by the ENMs. However, the turbulent flow of water over the surface apparently prevents the formation of a close particle layer. This is the reason why neither the flux declines nor pressure difference increases.

On the other hand the present nanoparticles in the feed which are less in concentration than the microparticles, are not able to form a coherent dense cake layer. They diffuse in the membrane but due to the high velocity of the feed they are not entrapped in the nanofibrous layer. Hence they only pass through the membrane.

It should be noted that the turbidity of permeated suspension decreases significantly with time. Most probably bigger agglomerates are formed due to instability of the surfactant layer around the particles under flow conditions. These agglomerates are rejected and do not take part in the filtration process any more. Consequently, the particle loading of the permeating suspension decreases. This kind

of big agglomerates whose size even exceeds several microns are observed in figs.12 B and D.

As mentioned earlier, when only the nanoparticles are present in the primary feed, at the onset of experiment, entrapment of nanoparticles by the nanofibers results in the increase of pressure difference. This high pressure difference could be a factor by which the nanofibrous layer is deformed. In fact, when the nanoparticles are involved, in addition to cake layer formation, deformation of the nanofibrous layer could also be influential in the loss of permeation flux.

As can be seen in fig. 13A, when only the nanoparticles are involved (d90≈ 560nm), the heat treated ENMs as single layer perform same as the un-treated ones. The only differences observed for the heat treated ENMs as compared to the un-treated ones are the complete rejection of the nanoparticles after a shorter time (1 hour) and the much lower primary pressure difference which then rises up significantly. Similar to the un-treated ENMs, the high retention performance costs the drastic decline of permeation flux and increase of pressure difference in a very short time (less than 1 hour) (figs. 13 B and C, respectively).

At first glance, the similarity of the rejection results for the un- and heat treated ENMs demonstrate that the dominant mechanism of pore blockage in the electrospun nanofibrous membranes is only cake layer formation. As mentioned earlier, heat treatment of the ENMs can preserve the integration of the nanofibrous layer during filtration. Hence, if deformation of the nanofibrous layer is the main or the supplementary reason (along with cake layer formation) for loss of flux, the heat treated ENMs should perform much better in term of permeation flux. Although, this interpretation seems reasonable, but also it should be noted that in the retention tests, pressure differences throughout the experiments was higher as compared to that in

water flux measurements. Hence, the supplementary effect of the structural deformation caused by high feed pressures to cake layer formation should be kept still in mind even for the heat treated membranes.

It is assumed that as soon as start of cake layer formation through entrapment of the nanoparticles in the nanofibrous layer, pressure difference increases by which the deformation happens. This process takes a shorter time for the un-treated ENMs and occurs almost at the onset of experiment. Deformation of the nanofibrous layer along with complete formation of the cake layer decrease the permeation flux. The lower primary pressure difference indicates that the heat treated ENMs can resist against deformation for a longer time but afterwards, pressure difference due to more development of cake layer increases so high that deformation is inevitable.

The investigations on the potential of the electrospun nanofibrous membranes for water treatment was done by several research groups such as Aussawasathien et al. [10] and Gopal et al. [11,12]. They could demonstrate that this kind of nanofibrous webs are able to act as an efficient membrane in separation of monodisperse particles. As a step further to meet more practical conditions, we tried to evaluate the filtration potential of PES electrospun nanofibrous web based composite membrane by using heterodisperse aqueous suspensions and at a longer time duration.

On the whole, the results showed that as water treatment, if the real suspensions to be filtered are considered to contain a diverse range of particle size including micro and nano particles, then the PES/PET ENMs act as an efficient pre-filter or even a microfiltration membrane. This situation due to agglomeration is not so impractical. These ENMs are able to remove the coarser particles (in this study; microparticles bigger than 1 micron) while keeping a high permeation flux. Also, the

smaller particles can pass through the membranes but they never clog the pores. These characteristics all meet the prerequisites of a suitable pre-filter [23].

4. Conclusion

Electrospun nanofibrous nonwovens due to their special structural features can be considered for filtration application. In the current study, applicability of PES electrospun nanofibrous mat supported by a PET sublayer for liquid filtration was investigated. Pure water flux measurements demonstrated the high permeability of this nanofibrous composite membrane. However, the deformation of the PES nanofibrous layer at high feed pressures could lower the water permeation. Heat treatment approach was adopted as an effective approach to enhance the integration of the composite membrane in order to prevent delamination and deformation of the nanofibrous layer. In a particle challenge test based on particulate aqueous suspensions, this nanofibrous composite membrane showed a high permeability while rejecting microparticles efficiently. However, in the case of nanoparticles much smaller than the average pore size, in spite of optimum rejection of the nanoparticles, the permeation declined drastically. Considering the characteristics of real particulate suspensions in water treatment, containing a mixture of micro- and nanoparticles, this electrospun nanofibrous membrane has the potential to be used in pre-treatment of water, one step before ultra- and nanofiltration membranes.

References

[1] Zheng-Ming Huang, Y.-Z. Zhang, M. Kotaki, S. Ramakrishna, A review on polymer nanofibers by electrospinning and their applications in nanocomposites, Composites Science and Technology 63 (2003) 2223–2253.

[2] H. Fong, D.H. Reneker, Elastomeric nanofibers of styrene–butadiene–styrene triblock copolymer, J. Polym. Sci. Part B: Polym. Phys. 37 (1999) 3488–3493.

[3] M. Bognitzki, W. Czado, T. Frese, A. Schaper, M. Hellwig, M. Steinhart,A. Greiner, H.J.Wendorff, Nanostructured fibers via electrospinning, Adv.Mater. 13 (2001) 70–72.

[4] X. Zong, K. Kim, D. Fang, S. Ran, B.S. Hsiao, B. Chu, Electrospun bioabsorbable nanofiber membranes, Polymer 43 (2002) 4403–4412.

[5] C. Burger, B. S. Hsiao, and B.Chu, Nanofibrous materials and their applications, Annu. Rev. Mater. Res. 36 (2006) 333–368.

[6] W.J. Wrasidlo, K.J. Mysels, The structure and some properties of graded highly asymmetrical porous membranes. J. Parenteral Sci Technol 38(1984) 24-31.

[7] F.G. Paulsen, S.S. Shojaie, W.B. Krantz, Effect of evaporation step on macrovoid formation in wet-cast polymeric membranes, J Membrane Sci. 91 (1994) 265-282.

[8] Kyunghwan Yoon, Kwangsok Kim, Xuefen Wang, Dufei Fang, Benjamin S. Hsiao, Benjamin Chu, High flux ultrafiltration membranes based on electrospun nanofibrous PAN scaffolds and chitosan coating, Polymer 47 (2006) 2434–2441.

[9] X. Wang, X. Chen, K. Yoon, D. Fang, B.S. Hsiao, B. Chu, High flux filtration medium based on nanofibrous substrate with hydrophilic nanocomposite coating, Environ. Sci. Technol. 39 (2005) 7684–7691.

[10] D. Aussawasathien, C. Teerawattananon, A. Vongachariya, Separation of micron to sub-micron particles from water: Electrospun nylon-6 nanofibrous membranes as pre-filters, J. Membrane Sci. 315 (2008) 11–19.

[11] R. Gopal, S. Kaur, Z. Ma, C. Chan, S. Ramakrishna, T. Matsuura, Electrospun nanofibrous filtration membrane, J. Membrane Sci. 281 (2006) 581–586.

[12] R. Gopal, S. Kaur, C.Y. Feng, C. Chan, S. Ramakrishna, S. Tabe, T.Matsuura, Electrospun nanofibrous polysulfone membranes as pre-filers:particulate removal, J. Membrane Sci. 289 (2007) 210–219.

[13] H. Fessi, F. Puisiex, J. P. Devissaguet, J. P. Ammoury and S. Betina, Nanocapsule formation by interfacial polymer deposition following solvent displacement, Int. J. Pharm., 55 (1989) R1-R4.

[14] K.Ebert, B.Maltzahn, R.Just, Verfahren zur Herstellung von Nanopartikeln unter Verwendung poröser Membranen. Deutsches Patent DE 10 2005 025 057

[15] S. Belfer, R. Fainchtain, Y. Purinson, O. Kedem, Surface characterization by FTIR-ATR spectroscopy of polyethersulfone membranes-unmodified, modified and protein fouled, J. Membrane Sci. 172 (2000) 113–124.

[16] Meng Wang, Li-Guang Wu, Xing-Cun Zheng, Jian-Xiong Mo, Cong-Jie Gao, Surface modification of phenolphthalein poly(ether sulfone) ultrafiltration membranes by blending with acrylonitrile-based copolymer containing ionic groups for imparting surface electrical properties, J. Colloid and Interface Sci. 300 (2006) 286–292.

[17] M. Mulder, Basic Principles of Membrane Technology, 2nd ed., Kluwer Academic, Boston, 1996.

[18] Zhan Wang, Dezhong Liu, Wenjuan Wu, Mei Liu, Study of dead-end microfiltration flux variety law, Desalination 201 (2006) 175–184.

[19] Phillip Gibson, Heidi Schreuder-Gibson, Donald Rivin, Transport properties of porous membranes based on electrospun nanofibers, Colloids and Surfaces A: Physicochemical and Engineering Aspects 187–188 (2001) 469–481.

[20] Ingmar H. Huisman, Benoît Dutrê, Kenneth M. Persson, Gun Trägårdh, Water permeability in ultrafiltration and microfiltration:Viscous and electroviscous effects, Desalination 113 (1997) 95-103.

[21] M. Nidhin, R. Indumathy, K. J. Sreeram and Balachandran Unni Nair, Synthesis of iron oxide nanoparticles of narrow size distribution on polysaccharide templates, Bull. Mater. Sci., 31(1) (2008) 93–96.

[22] J.R. Alvarez, Pressure driven membrane processes, in: J. Coca, S. Luque (Eds.), Membrane Applications in the Food and Dairy Industry, University of Oviedo, Spain, 1999, pp. 23–42.

[23] R.W. Baker, Membrane Technology and Applications, 2nd ed., Wiley, 2004.

Table captions

Table 1. Electrospinning conditions

Table 2. PES nanofiber mat properties

Table 3. Band assignments for the infrared spectrum of PES [15]

Table 4. PES/PET composite membrane properties

Figure captions

Figure 1. Two-tier structure of PES/PET composite membranes

Figure 2. The custom-built set-up used for permeability and retention tests

Figure 3. SEM micrographs showing morphology of the PES electrospun nanofibers

Figure 4. SEM micrographs showing the improved adhesion of the fibers at the interface

Figure 5. ATR-FTIR spectra of A) the heat treated PES nanofibers in air B) the untreated PES nanofibers

Figure 6. Thermogravimetric analysis (TGA) curves of A) as-received PES B) heat treated PES nanofibers and C) un-treated PES nanofibers

Figure 7. Permeability characterization of the PES/PET membranes A) Pure water flux and ; B) Pressure difference over the membranes

Figure 8. The surface of three consecutive layers of PES/PET membrane (multi layer) after filtration A) the uppermost layer- deformation of the nanofibrous layer is obvious B) the second layer C) the third layer

Figure 9. Interfiber adhesion makes the nanofibrous layer rigid enough to resist against deterioration by water flow

Figure 10. Heat treatment prevents deformation of the nanofibrous layer A) surface of the uppermost layer of the un-treated PES/PET membrane after filtration B) surface of the uppermost layer of the heat-treated PES/PET membrane after filtration C) cross section of the uppermost layer of the un-treated PES/PET membrane after filtration D) cross section of the uppermost layer of the heat-treated PES/PET membrane after filtration

Figure 11. The retention performance of the PES/PET ENMs A) d90 of the particles present in the permeates indicating retention ability of the membranes B) permeation flux of the membranes during measurements C) pressure difference over the membranes during measurements (PS: particle size)

Figure 12. A&B) The cake layer formed at the surface of the PES/PET membranes when the particle size is below 1μm at different magnifications C & D) The particles (over 1μm in size) rejected by the membranes does not form a dense and coherent cake layer at different magnifications

Figure 13. The retention performance of the PES/PET ENMs A) d90 of the particles present in the permeates indicating retention ability of the membranes B) permeation flux of the membranes during measurements C) pressure difference over the membranes during measurements

Tables:

Table 1

PES Concentration	20 wt%
Applied voltage	20 kV
Feed rate	0.5 mL/h
Spinning distance	25 cm
Collection time	8 h
Inner diameter of the needle	0.8 mm

Table 2

Morphology of the nanofibers	Smooth surface, no beads and droplets
Diameter of the nanofibers	260 ±110 nm
The thickness of the PES nanofibrous mat	100 ±30 μm

Table 3

Wavenumber (cm^{-1})	Assignment
3095	aromatic C-H vibration
1575,1483	aromatic band (C=C ring)
1404	CH$_2$ bond
1320	asymmetric vibrations of the SO$_2$ group
1296	Vibrations of the SO$_2$ group
1234	C–O ether
1145	Symmetric vibrations of the SO$_2$ group
1101	aromatic ring
1070	Symmetric vibrations of SO$_3^-$
1010	Un-known
870,832,797,698	C-H bending vibrations
717	CH$_2$ bond

Table 4

Thickness	200 μm
Areal density	0.2-0.3 g/cm^2
Active filtration area	$\approx$0.001 m^2
Mean flow pore diameter	2 μm
Bubble point pore diameter	5 μm

Figures:

PES electrospun nanofibers

PET non-woven
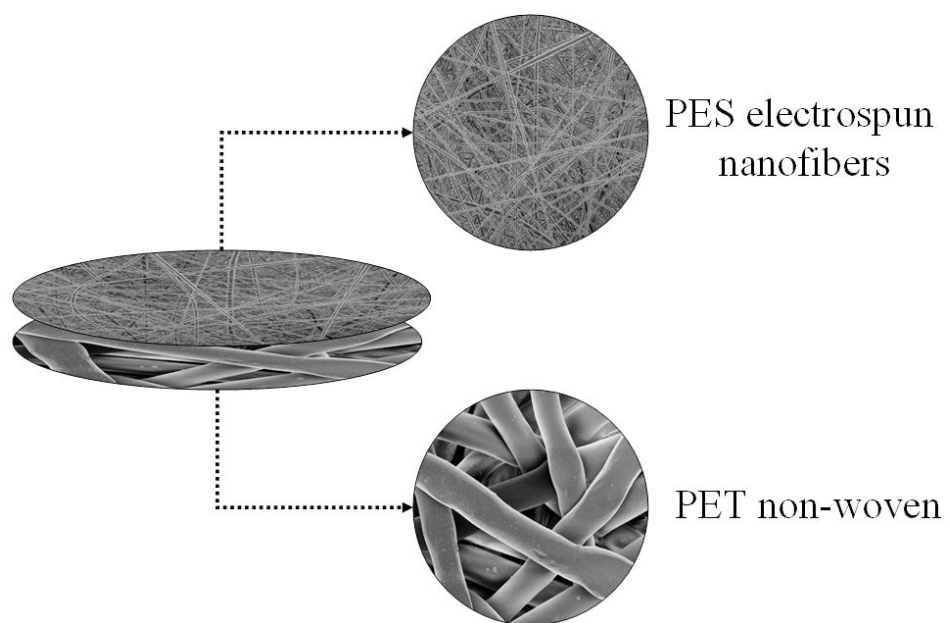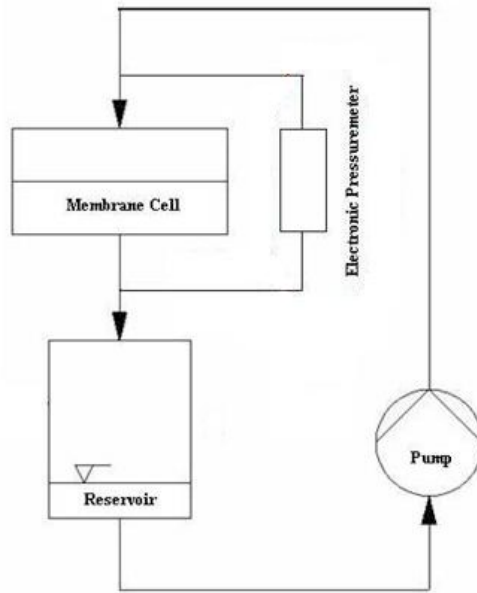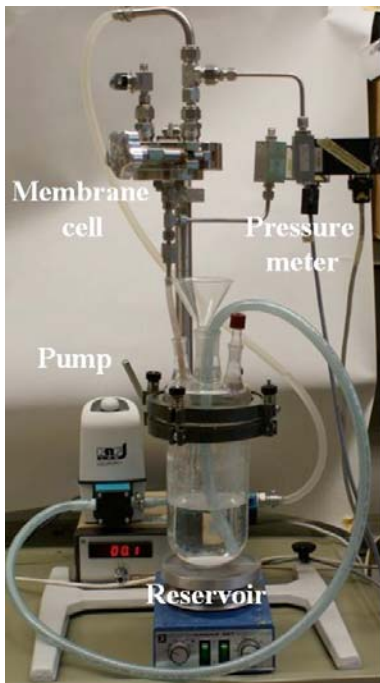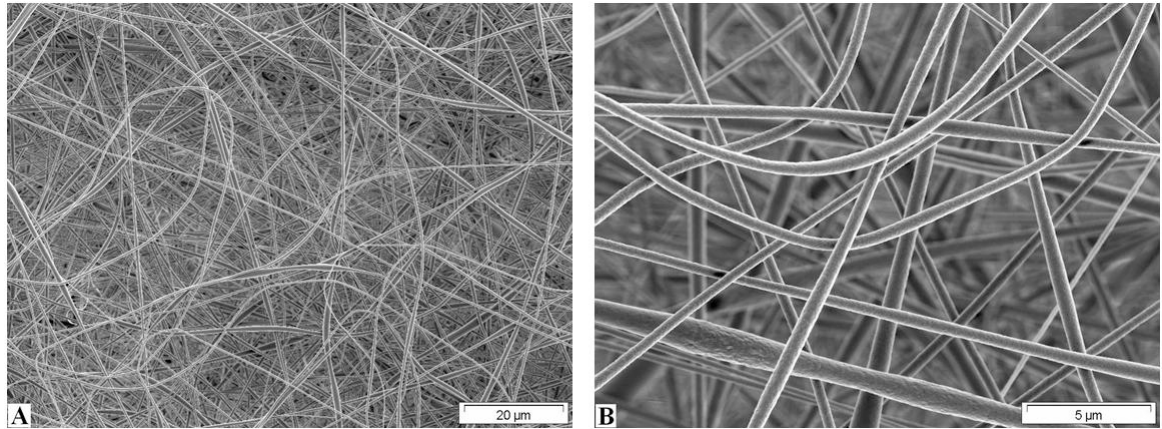
Figure 1

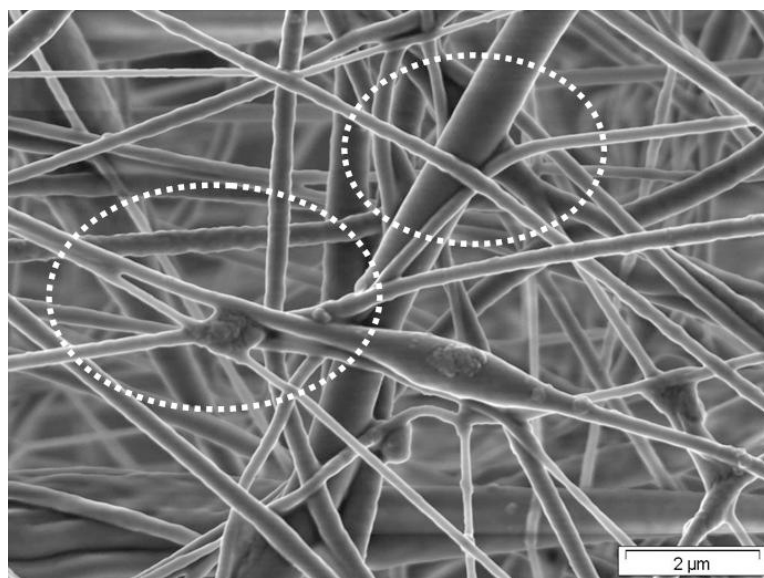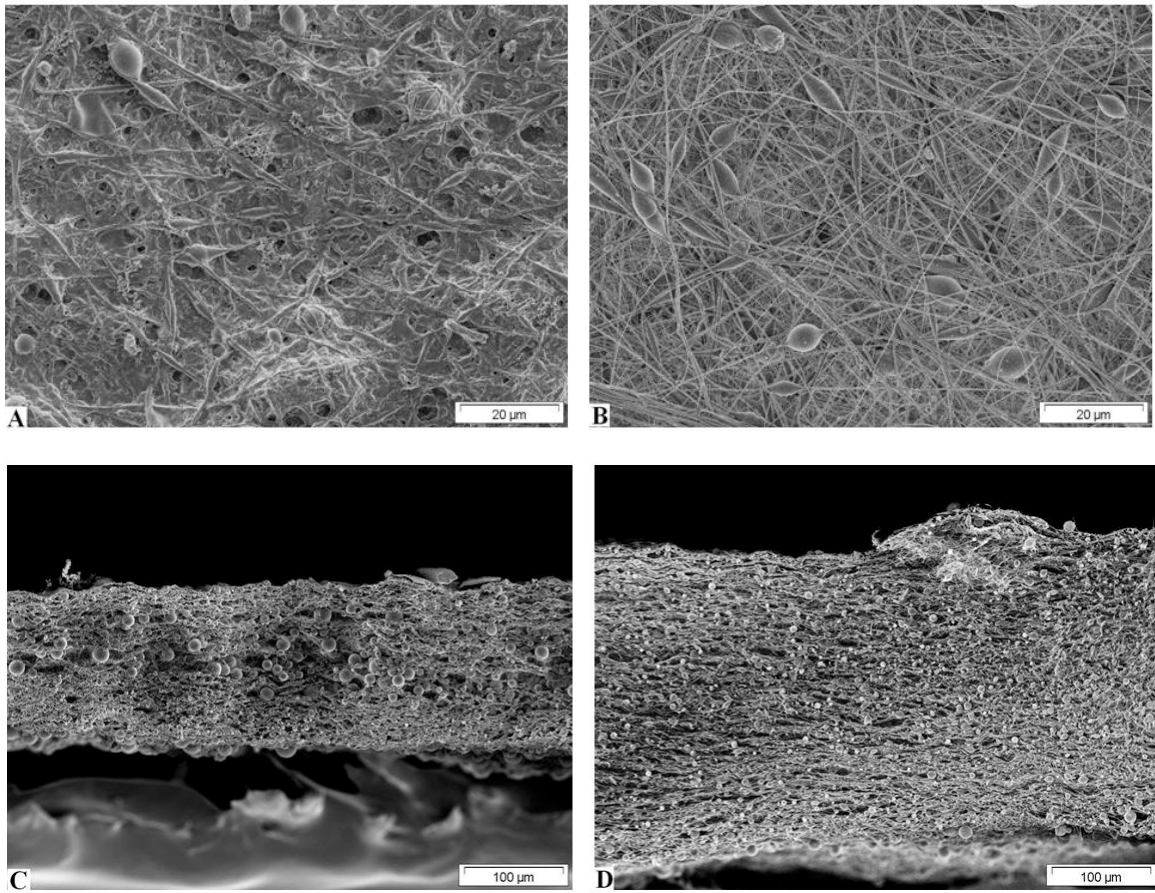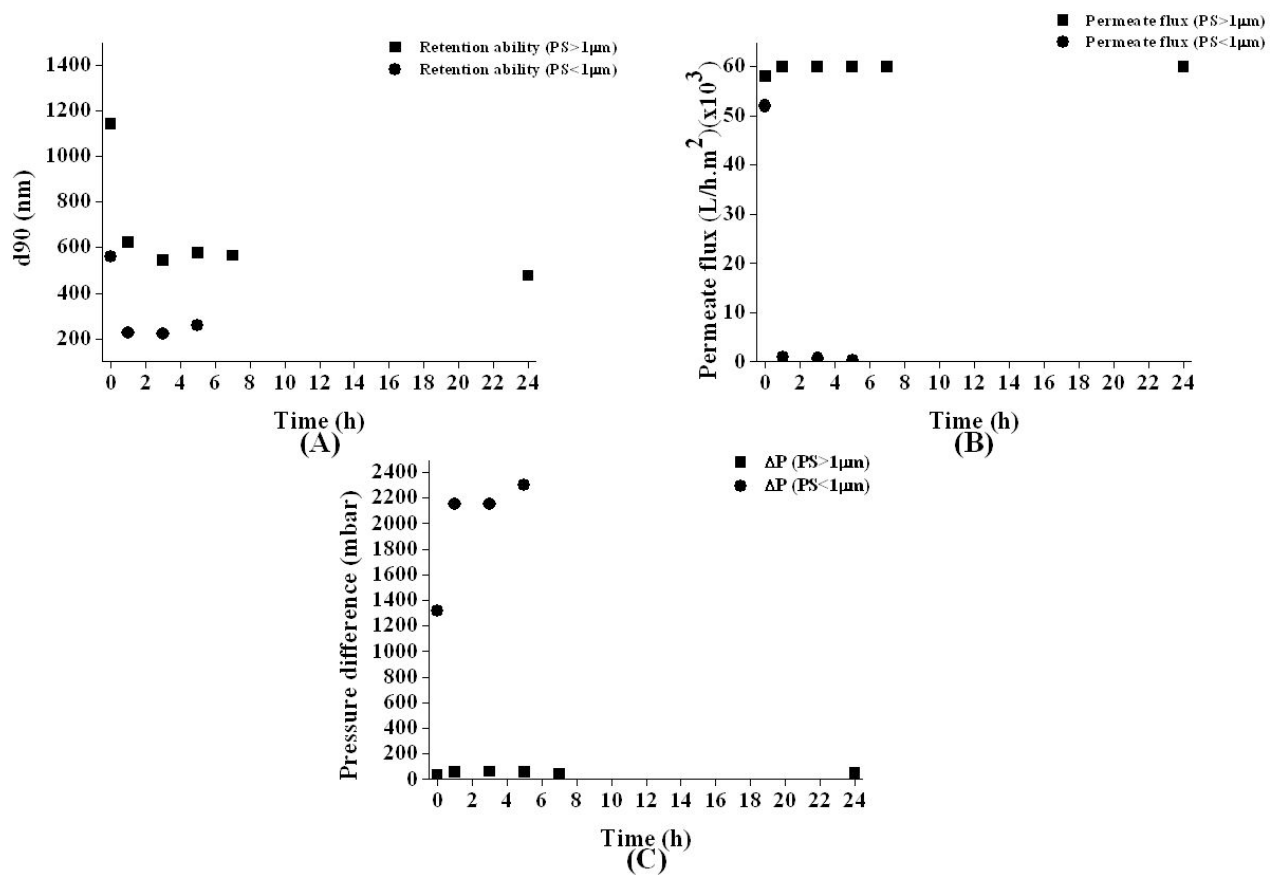Figure 2
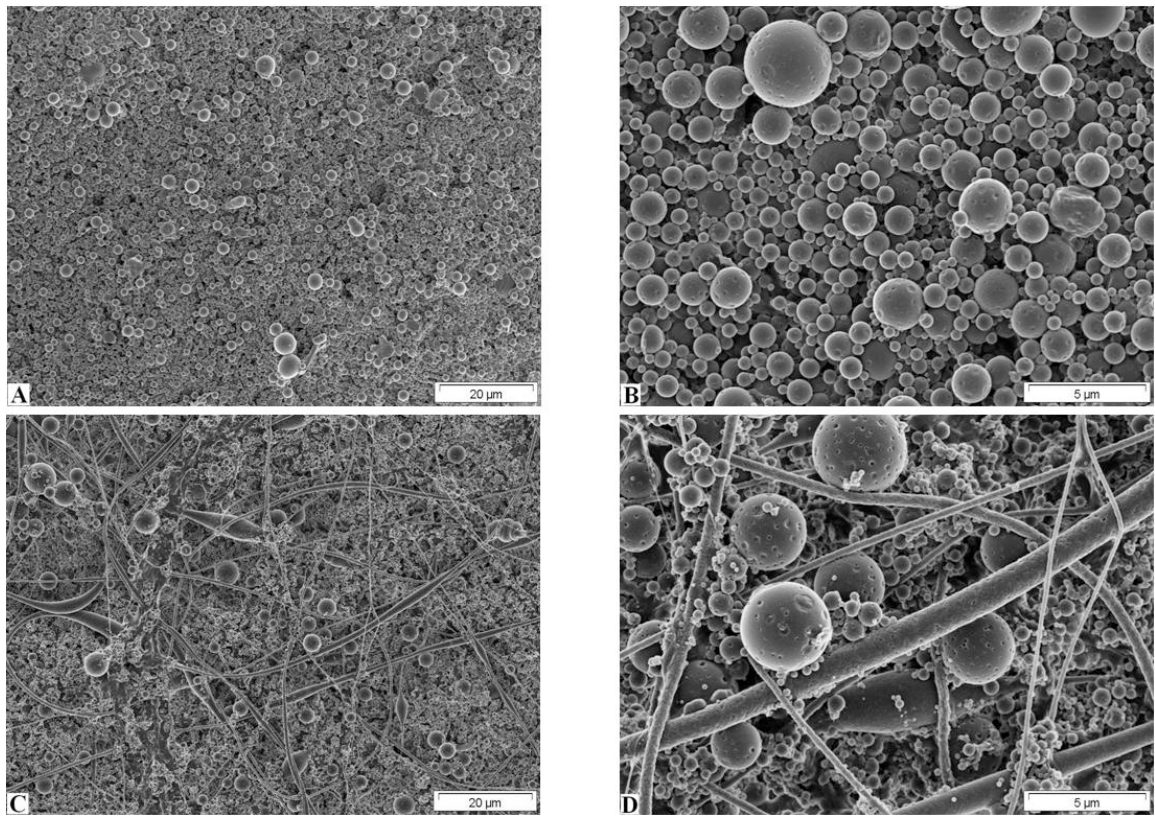
Figure 3
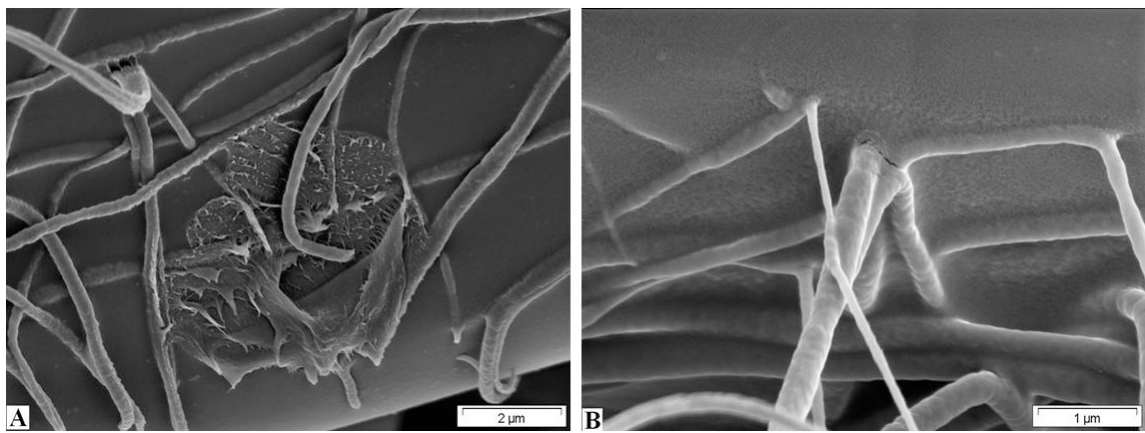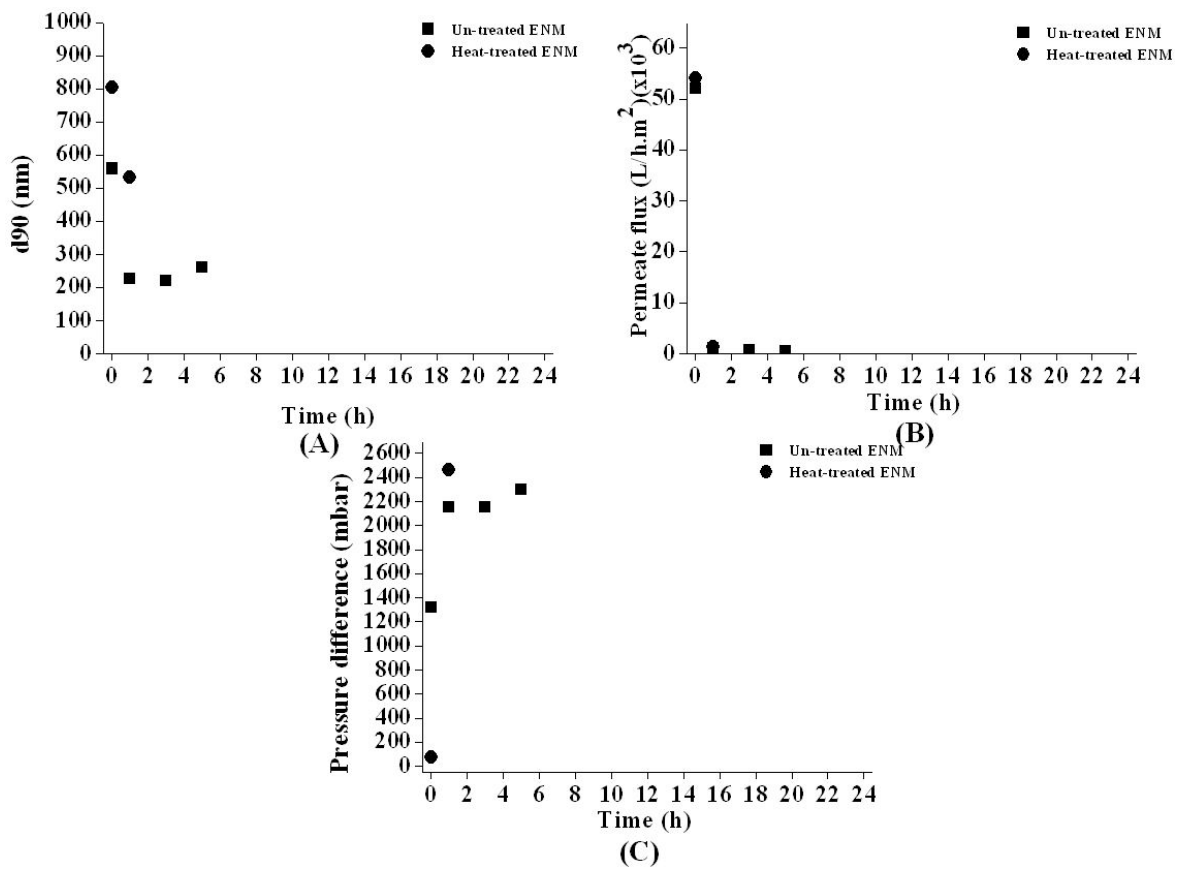
Figure 4
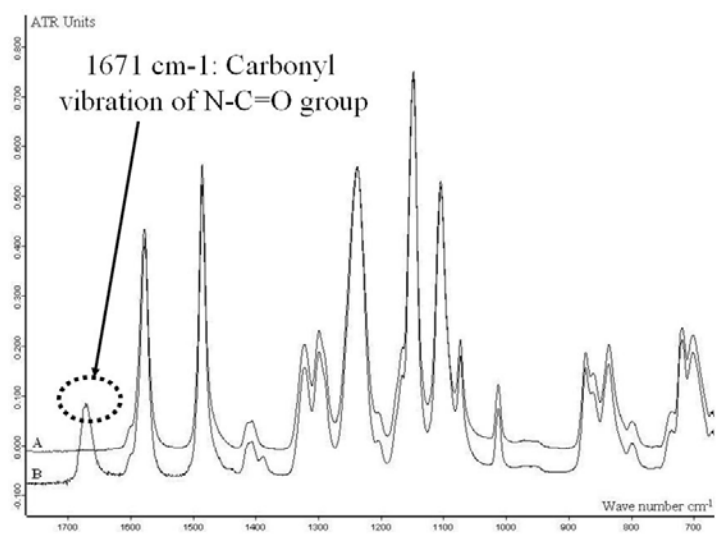
Figure 5
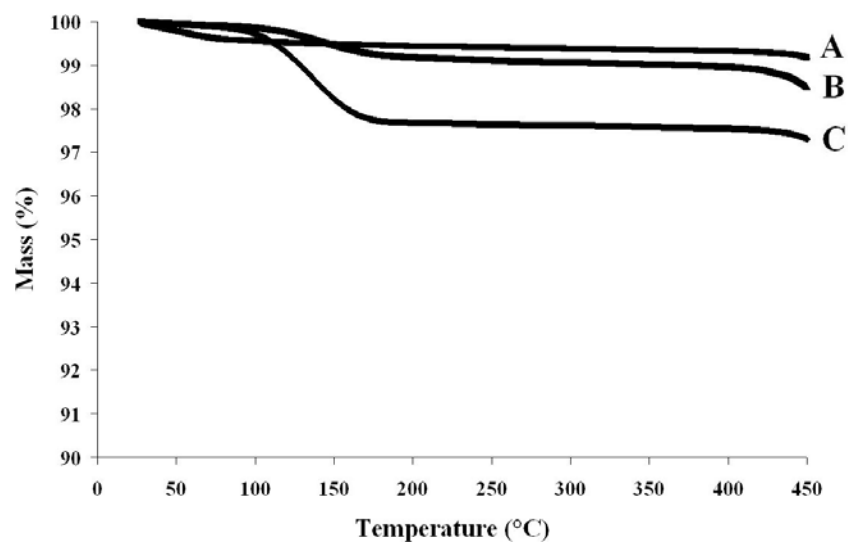
Figure 6
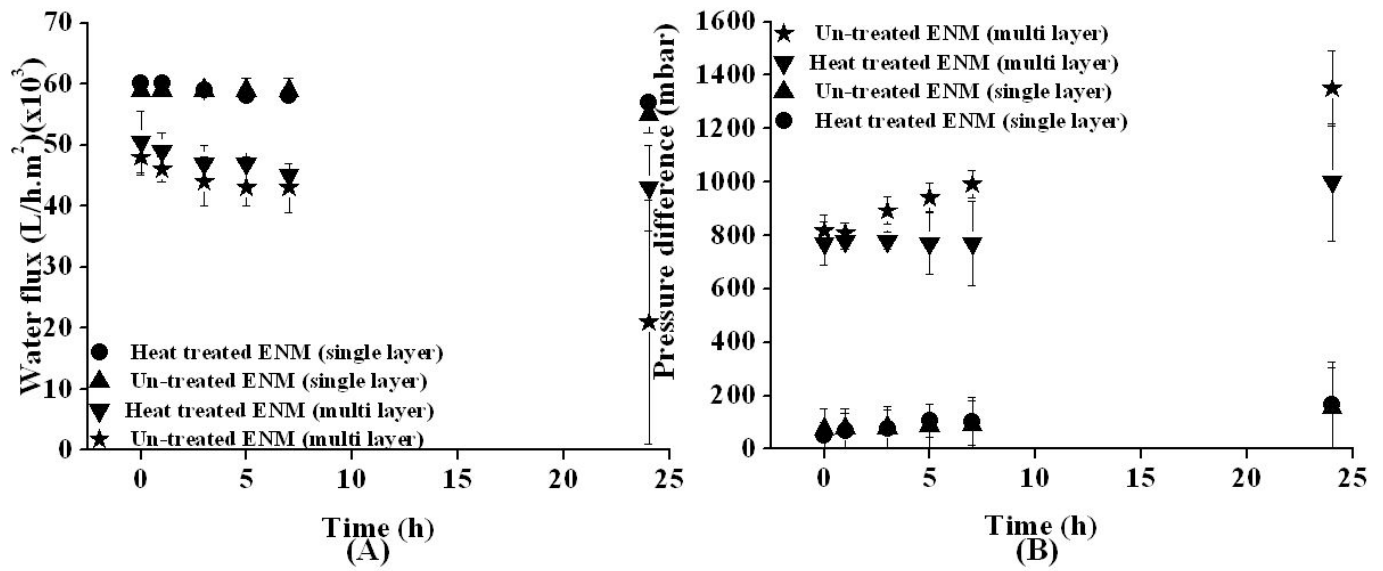
Figure 7
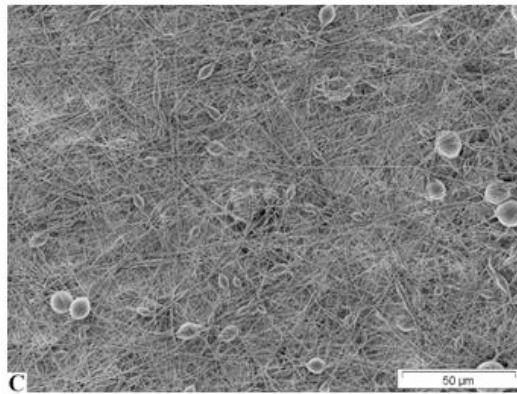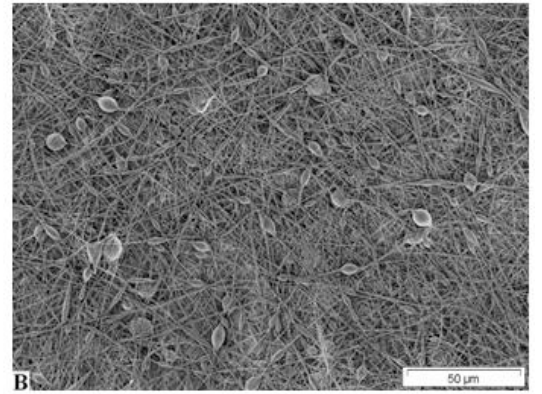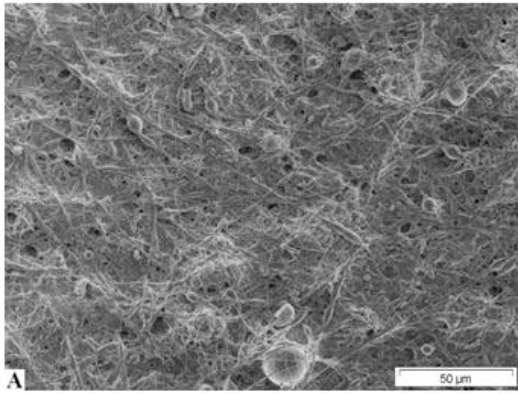
Figure 8

Figure 9

Figure 10

Figure 11

Figure 12

Figure 13